Research Article

Marco Klute*, Alexander Piontek, Hans-Peter Heim and Stephan Kabasci

Effects of blending poly(lactic acid) and thermoplastic polyester polyurethanes on the mechanical and adhesive properties in two-component injection molding

https://doi.org/10.1515/ipp-2021-4212
Received December 17, 2021; accepted July 21, 2022;
published online September 16, 2022

Abstract: One possible way to increase the use of bioplastics and thus contribute to a more resource-efficient and sustainable economy is to broaden the application range of such bioplastics. Poly(lactic acid) (PLA) is a promising and commercially available bio-based and biologically degradable polymer, which exhibits a high strength and stiffness but is very brittle. Blending with other polymers can lead to an enhancement of the ductility of the PLA. The goal of this work was to show that blending of PLA with a bio-based thermoplastic polyester-urethane elastomer (TPU) increases the ductility of the compound and also affects the adhesion of the layers when the materials – the modified PLA compound and the TPU – are processed via two-component (2C) injection molding to form corresponding composite parts. The results show that both goals – the increased ductility as well as the increased adhesion between the polymeric phases in 2C parts – can be reached by compounding PLA with two different bio-based polyester-based TPUs. Tensile strength and Young's modulus of the compounds decrease according to a linear mixing rule with the addition of TPU. Elongation at break and notched Charpy impact strength increase by 750 and 200%, respectively. By addition of the TPU, the surface free energies of the compounds were increased, especially the polar parts. This led to reduced interfacial tensions between the produced compounds and the neat TPUs and thus increased the adhesion between them. For the softer TPU the adhesion was so strong that the TPU showed a cohesive failure in the 90° peel test and thus could not be separated from the compound substrate at all. For the harder TPU the bonding strength increased by 140% upon the addition of this TPU inside the hard component.

Keywords: biopolymers; compatibilization; interfacial tension; peel tests; two-component injection molding.

***Corresponding author: Marco Klute**, University of Kassel, Institute of Material Engineering - Polymer Engineering, Mönchebergstr. 3, 34125 Kassel, Germany, E-mail: marco.klute@uni-kassel.de
Alexander Piontek and Stephan Kabasci, Fraunhofer UMSICHT, Institute for Environmental, Safety and Energy Technology, Osterfelder Str. 3, 46047 Oberhausen, Germany, E-mail: alexander.piontek@umsicht.fraunhofer.de (A. Piontek), stephan.kabasci@umsicht.fraunhofer.de (S. Kabasci)
Hans-Peter Heim, University of Kassel, Institute of Material Engineering–Polymer Engineering, Mönchebergstr. 3, 34125 Kassel, Germany, E-mail: heim@uni-kassel.de

1 Introduction

In the past years, consumers as well as the plastics industry have significantly increased their awareness regarding the sustainability of conventional fossil-based plastics versus bioplastics, which include both bio-based and biodegradable plastics (Filho et al. 2021). Furthermore, this awareness has reached governmental consideration and manifests within the Green Deal of the European Comission (EC) (European Commission 2019) as well as within the United Nations'(UN) Sustainable Development Goals (United Nations 2015). With regard to the aims of the EC and the UN, the use of bioplastics can be one way to reach a more resource-efficient and circular economy (Di Bartolo et al. 2021; Spierling et al. 2018). To achieve this, it is necessary to broaden the field of applications for bioplastics as well as to implement specialized bioplastic compounds on the market that target specific applications.

Currently, the most established market for bioplastics is the area of packaging, where more than half of the produced bioplastics are used (European Bioplastics, 2021; Institute for Bioplastics and Biocomposites 2020). Major drawbacks of bioplastics are their insufficient material properties in contrast to their fossil-based counterparts

that had been established and specialized over the past decades. Thus, the application of bioplastics in areas such as technical parts is hindered (Pilla 2011).

There are several strategies to overcome these disadvantages with the aim to broaden the application range of bioplastics and many studies covered this topic (Nakajima et al. 2017). One established strategy is the compounding of biopolymers with other polymers to achieve material properties that are suitable for engineering applications (Wang et al. 2016a). A promising bio-based material that can be used for engineering applications is poly(lactic acid) (PLA). It shows good mechanical properties such as a high tensile strength and modulus, but on the other side is very brittle (Garlotta 2001). There are many publications available in which PLA is blended with other (bio-)polymers to overcome its inherent brittleness and achieve better material properties (Hamad et al. 2018). Examples are blends with PMMA (Anakabe et al. 2015), ABS (Cao et al. 2019), TPEE (Wang et al. 2016b), PA (Rasselet et al. 2019), PCL (Przybysz-Romatowska et al. 2020), EPDM (Piontek et al. 2020), PP (Kang et al. 2015), PET (Gere and Czigany 2020), PBS (Su et al. 2019), or TPU (Bernardes et al. 2020). In addition to the improved mechanical characteristics, the blending of PLA with other polymers affects its crystallization behavior resulting in an enhancement of the cold crystallization enthalpy and an accelerated crystallization during cooling (Yokohara and Yamaguchi 2008). In regards of producing more complex parts for engineering applications in injection molding processes with PLA, the accelerated crystallization enables shorter cooling times leading to cycle times that are competitive with the fossil-based counterparts.

One processing method with increasing attention for engineering applications is multicomponent injection molding. This process enables the creation of form-fitting joints of two or more polymers in one process without further postprocessing like welding or gluing. Injection molded plastic-plastic composites are mainly produced to combine material properties, such as color, hardness, or viscosity as well as thermal and electrical properties (Mieth and Tromm 2016). By combining properties, it is possible to integrate specific functions in the component or to link functional elements. For example, in hard-soft composites, the hard component absorbs loads, while the soft component usually acts as damping or sealing or it fulfills haptic functions (Klute et al. 2018; Rüppel 2021; Schlitt et al. 2019).

The aim of this study was to show that the blending of PLA not only enhances its mechanical properties and processability but also improves the adhesive properties in two-component (2C) injection molded parts to create stronger material bonds between the hard and soft components. The supposed mechanism behind this assumption is illustrated in Figure 1, where light green represents a commercially available PLA based blend and orange the TPU. Prior to the 2C injection molding of a soft plastic onto a hard one, the two materials are blended in a compounding process to create a hard component that contains small amounts of the soft component (middle of Figure 1). During the overmolding of this blend, the soft component will connect with the small inclusions of soft component in the blend to create a stronger bond.

Both steps will be addressed separately in terms of process parameters and characteristics. During compounding, it is crucial to achieve a homogeneous distribution of

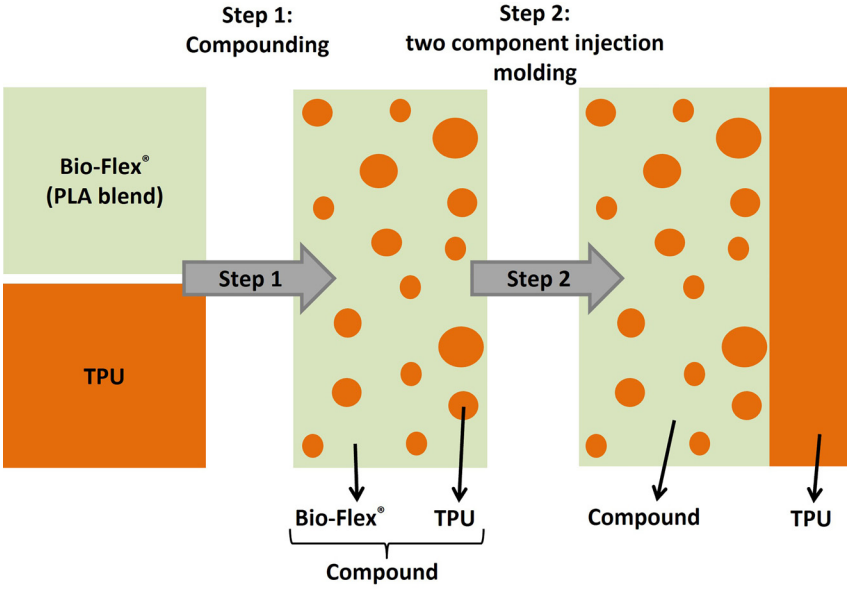

Figure 1: Schematic illustration of the approach of this study.

the TPU in the PLA blend. This distribution and the morphology of the compounds will be analyzed using scanning electron microscopy (SEM) and differential scanning calorimetry (DSC). To increase the bonding strength of the 2C parts as shown in Figure 1, the small amount of TPU within the compound needs to be present at the surface onto which the soft component will be injected.

When processing PLA in two-component injection molding for producing hard-soft composites with TPU, the interfacial tension is an important parameter that determines the creation of a strong adhesive bonding. Studies have shown that a small interfacial tension between the hard and the soft component leads to high bonding strengths of the material joints (Güzel et al. 2020). Since the calculated interfacial tension (IFT) between identical materials is zero, higher amounts of TPU on the compound's surface will lead to lower interfacial tensions between the compound and the TPU soft component. This will be analyzed using drop shape analysis (DSA).

2 Experimental

2.1 Materials

A Poly(lactic acid) based blend (Bio-Flex® S7514) was kindly provided by FKuR Kunststoffe GmbH, Willich, Germany. It is characterized by a melt flow index (MFI) of 24 g per 10 min (210 °C, 2.16 kg) and consists of PLA blended with a second bio-based polyester. Thermoplastic polyester urethane elastomers (TPU, Elastollan® N75A12 P, Elastollan® N95A12, abbreviated as N75A and N95A, respectively) were kindly provided by BASF Polyurethanes GmbH, Lemförde, Germany, with shore hardnesses of 75 and 95 A and bio-based carbon contents of 49 and 43%, respectively. For the characterization of the surface free energy, two test liquids with known surface tensions had to be used. For this purpose, water (H_2O) and Diiodomethane (CH_2I_2) (Sigma-Aldrich, St. Louis, MO, USA) were used since several studies showed their applicability for the characterization of PLA based biopolymers (Bernardes et al. 2020; Chen and Zhen 2021).

2.2 Sample preparation

The PLA/TPU blends were compounded with a co-rotating twin-screw extruder (ZSK 25 from Coperion GmbH, Stuttgart, Germany, screw diameter 25 mm, L/D ratio 40) at different mass ratios (95/5, 90/10, 85/15, 80/20) and are denoted as x-N75A and x-N95A, where x corresponds to the mass percent of the corresponding TPU. Compounding was carried out with a screw speed of 300 rpm and a mass flow rate of 15 kg/h. The temperature profiles are shown in Table 1. The extruder contains an atmospheric degassing, a two hole nozzle with a diameter of 3 mm each, a water bath for cooling and a strand pelletizer. The raw materials were dried at 60 °C in a dry-air dryer overnight before processing. The prepared compounds were dried in the same way.

The process ing parameters screw speed, mass temperature and torque were recorded during the compounding. With these parameters, the specific mechanical energy consumption (SMEC) can be calculated according to Eq. (1) (Rauwendaal 2014).

$$SMEC\left[\frac{kJ}{kg}\right] = \frac{2\cdot\pi\cdot 60\cdot n\cdot M_D}{\dot{m}}. \quad (1)$$

Therein n is the screw speed in min^{-1}, M_D is the torque of the extruder ram in Nm and $\dot{m}$ is the mass flow rate in kg/h.

For the characterization of the mechanical properties of the produced blends and the TPU, tensile test specimens (type 1A for the blends and type S2 for the TPU) were produced according to ISO 527-2 (1A) and DIN 53,504 (S2) using an injection molding machine (Arburg Allrounder 320C Golden Edition from Arburg GmbH + Co KG, Loβburg, Germany). The processing parameters were set according to Table 2.

To test the bonding strength of the materials, two-component peel test specimens were produced according to the test guideline VDI 2019 of the Association of German Engineers (VDI Verein Deutscher Ingenieure e.V., Düsseldorf, Germany). For this overmolding, a two-component injection molding machine (Arburg Allrounder 470S from Arburg GmbH + Co KG, Loβburg, Germany) with two injection units was used. The production process consists of two consecutive steps. First,

Table 1: Temperature profile in the compounding extruder.

Samples containing	Zone 1 (Hopper) [°C]	Zone 2/3 [°C]	Zone 4 [°C]	Zone 5 [°C]	Zone 6 [°C]	Zone 7/8 [°C]	Zone 9/10 [°C]	Zone 11 (Die) [°C]
N75A	60	170	180	180	180	180	180	180
N95A	66	170	180	190	190	190	190	190

Table 2: Processing parameters for the injection molding of tensile test specimen.

Process parameters	Blend	TPU
Melt temperature [°C]	180	220
Mold temperature [°C]	30	30
Injection velocity [cm³/s]	32	50
Injection pressure [bar]	800[a]	600[a]
Packing pressure [bar]	600/500/100	400/50
Packing time [s]	3/4/1	1/4
Cooling time [s]	30	25

[a]Approximate values, the pressure varies depending on the shore hardness of the TPU and the amount of TPU in the blend.

Table 3: Processing parameters for the injection molding of 2C peel test specimen.

Process parameters	Injection unit 1	Injection unit 2
Melt temperature [°C]	180	200
Mold temperature [°C]	30	30
Injection velocity [cm³/s]	50	50
Packing pressure [bar]	600/25	25
Packing time [s]	2/1	1
Cooling time [s]	15	25

the PLA blend is injected to form the 40 mm wide substrate plate. After a defined cooling time a movable core opens the second cavity of the mold so that the TPU can be directly injected onto the substrate plate and an adhesive substance-bonded connection is formed. The dimensions of the peel specimens are shown in Figure 2 and the parameters used for injection molding are given in Table 3.

2.3 Characterization

2.3.1 Thermal and rheological properties

Differential scanning calorimetry (DSC) was performed with a DSC 204 F1 Phoenix from Erich NETZSCH GmbH & Co. Holding KG, Selb, DE, equipped with a liquid nitrogen cooling system. The device is regularly calibrated using an indium standard. The samples were cooled to –100 °C, held for 5 min, heated up to 230 °C, held for 3 min, cooled to –100 °C, held for 5 min and heated up to 250 °C. All heating and cooling rates were set to 10 K/min and the measurements were performed in a nitrogen atmosphere.

MFI measurements were performed using a Ceast Melt Flow 7026 from Instron GmbH, Darmstadt, Germany, at 210 °C using a weight of a mass of 2.16 kg.

2.3.2 Surface characterization

As mentioned before, the surface free energy (SFE) of the materials and the interfacial tension (IFT) between them significantly affect the adhesive bonding strength of injection molded 2C-compounds. We measured the SFE of the materials used in this study via the Drop Shape Analysis (DSA). For this method, a drop of a test liquid with known surface tension is placed on the surface of a substrate plate. Two three-phase angles between the solid plate, the liquid drop, and the surrounding gas are determined (Figure 3). For using water as the test liquid a contact angle between 1° and 90° is considered to result from good to partial wetting abilities, while 0° resembles a complete wetting (Rüppel et al. 2017).

The SFE of the solid substrate plate (σ_s) can be described using the Young's equation Eq. (2). The method of Owens, Wendt, Rabel and Kaelble (OWRK) (Kaelble 1970) extends the relationship between the SFE of the solid and the surface tension of the liquid drop (σ_l) by the dispersive (σ_s^D and σ_l^D) and polar (σ_s^P and σ_l^P) SFE parts of the two materials Eq. (3) (Kloubek 1992).

$$\sigma_s = \sigma_{sl} + \sigma_l \cdot \cos\theta, \tag{2}$$

$$\sigma_{sl} = \sigma_s + \sigma_l - 2\left(\sqrt{\sigma_s^D \cdot \sigma_l^D} + \sqrt{\sigma_s^P \cdot \sigma_l^P}\right). \tag{3}$$

By combining Eq. (2) and Eq. (3) and using the contact angles measured by means of two different test liquids with known surface tensions, the SFE of the substrate material

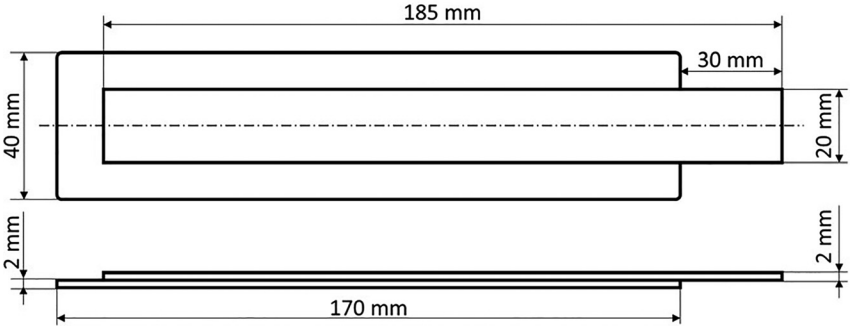

Figure 2: Dimensions of peel test specimen according to VDI 2019 guideline.

Figure 3: Two three-phase angles of a water drop on a PLA blend substrate surrounded by air.

can be calculated and divided into its dispersive and polar parts. In addition, the interfacial tension (σ_{sl}) between the two materials combined to an adhesive material bond in 2C injection molding can also be calculated using Eq. (3).

The DSA measurements on the injection molded substrate plates were carried out with a contact angle measuring device (EasyDrop DSA 20B, Krüss GmbH, Hamburg, Germany). As test liquids, water (H_2O) and diiodomethane (CH_2I_2) were used. The surface tensions of these liquids used to calculate the SFE of the substrate are given in Table 4. On every surface, the contact angles of ten drops of each liquid were measured and the mean values of those ten drops were used for the calculation of the SFE.

2.3.3 Morphological properties

Scanning electron microscopy (SEM) was performed with a Vega3 from TESCAN GmbH, Dortmund, Germany, with 20 kV acceleration voltage. The specimens were submerged in liquid nitrogen for 10 min and were then cryogenically broken. To prevent electrostatic charging, the fractured surfaces were sputter coated with gold under vacuum prior to observation.

2.3.4 Mechanical properties

Tensile tests of the hard phase were performed with a 5567A universal testing system from Instron GmbH, Darmstadt, Germany, at a speed of 50 mm/min in accordance with DIN EN ISO 527-1. Testing speed for the determination of the Young's modulus between 0.05 and 0.25% elongation was 1 mm/min. All results presented are averages from five measurements. Graphs of tensile tests represent the measurement with the median in elongation at break.

Charpy impact fracture tests of the hard phases were performed with a Ceast 9050 pendulum impact testing machine from Instron GmbH, Darmstadt, Germany, with notched (type A) specimens using a 5 J instrumented pendulum and unnotched specimens using a 15 J instrumented pendulum according to DIN EN ISO 179-2. All results presented are averages from 10 measurements.

The tensile tests of the TPU were performed using an Inspekt Table 5 kN universal testing system (Hegewald & Peschke Meβ-und Prüftechnik GmbH, Nossen, Germany). The testing speed was set to 200 mm/min in accordance with DIN EN ISO 527-1. For each material, eight specimens were tested. To perform the peel tests according to the VDI 2019 guideline, the universal testing system was equipped with a test trolley in which the substrate plate was fixed. The trolley allows a horizontal movement to ensure a 90° peel angle of the TPU over the guide pulley. The peeling speed was set to 100 mm/min and five test specimens of each material combination were tested.

The shore hardness of the TPU was measured using a digitest II hardness tester (Bareiss Prüfgerätebau GmbH, Oberdischingen, Germany). To ensure the thickness of 6 mm, three tensile test specimens were stacked and measured according to DIN ISO 7619-1 with a Shore A indenter. Five measurements for each TPU were performed with a testing time of 3 s.

For every measurement performed in this study, test specimens were stored under standard conditions (23 °C, 50% relative humidity) for at least 16 h prior to testing.

3 Results and discussion

3.1 Compounding

Compounding of the materials showed some differences between the blends containing the soft TPU N75A and the

Table 4: Surface tension of the two used test liquids.

Liquid	Surface tension [mN/m]	Polar component [mN/m]	Dispersive component [mN/m]	Source
Water	72.8	51.0	21.8	Janczuk and Bialopiotrowicz (1989)
Diiodomethane	50.8	2.3	48.5	Fowkes (1964)

Table 5: Mean values and standard deviation of the measured compounding parameters.

Sample	Speed [min^{-1}]	Torque[a] [%]	Mass temperature [°C]	SMEC [kJ/kg]
Ref	–	–	–	–
5-N75A	300 ± 1.5	48 ± 1.0	195 ± 0.5	589 ± 12
10-N75A	300 ± 1.2	48 ± 0.8	195 ± 0.4	590 ± 10
15-N75A	300 ± 1.1	48 ± 0.8	195 ± 0.4	597 ± 11
20-N75A	300 ± 1	48 ± 1.1	196 ± 0.5	598 ± 14
5-N95A	300 ± 1.5	50 ± 1.0	197 ± 0.5	616 ± 13
10-N95A	300 ± 1.4	51 ± 1.2	198 ± 0.7	630 ± 15
15-N95A	300 ± 1.4	52 ± 1.0	199 ± 0.9	645 ± 13
20-N95A	300 ± 1.3	53 ± 1.0	200 ± 1.2	651 ± 13

[a]Maximum torque of the extruder ram is 82 Nm.

blends containing the harder TPU N95A. The measured compounding parameters and their standard deviation are shown in Table 5. In total, the processing did not reveal noticeable deviations and thus was considered stable. From the results, it can be seen that the mass temperature increases with increasing content of the TPU inside the blends as well as with using the harder TPU type. The SMEC stays constant at the addition of N75A to the compound, but increases upon the addition of N95A and thus shows a similar behavior as the mass temperature. The higher SMEC values for N95A blends result from a higher viscosity that leads to an increased energy dissipation inside the polymer melt.

3.2 Thermal and rheological properties

Figure 4 depicts the cooling as well as the second heating curves of the produced samples, from which the melting and crystallization temperatures of the PLA phase can be deduced. It can be seen that the crystallization of the PLA shifts to lower temperatures and the crystallization enthalpy values decrease. Additionally, the temperature of the first melting peak of the PLA decreases with an increasing

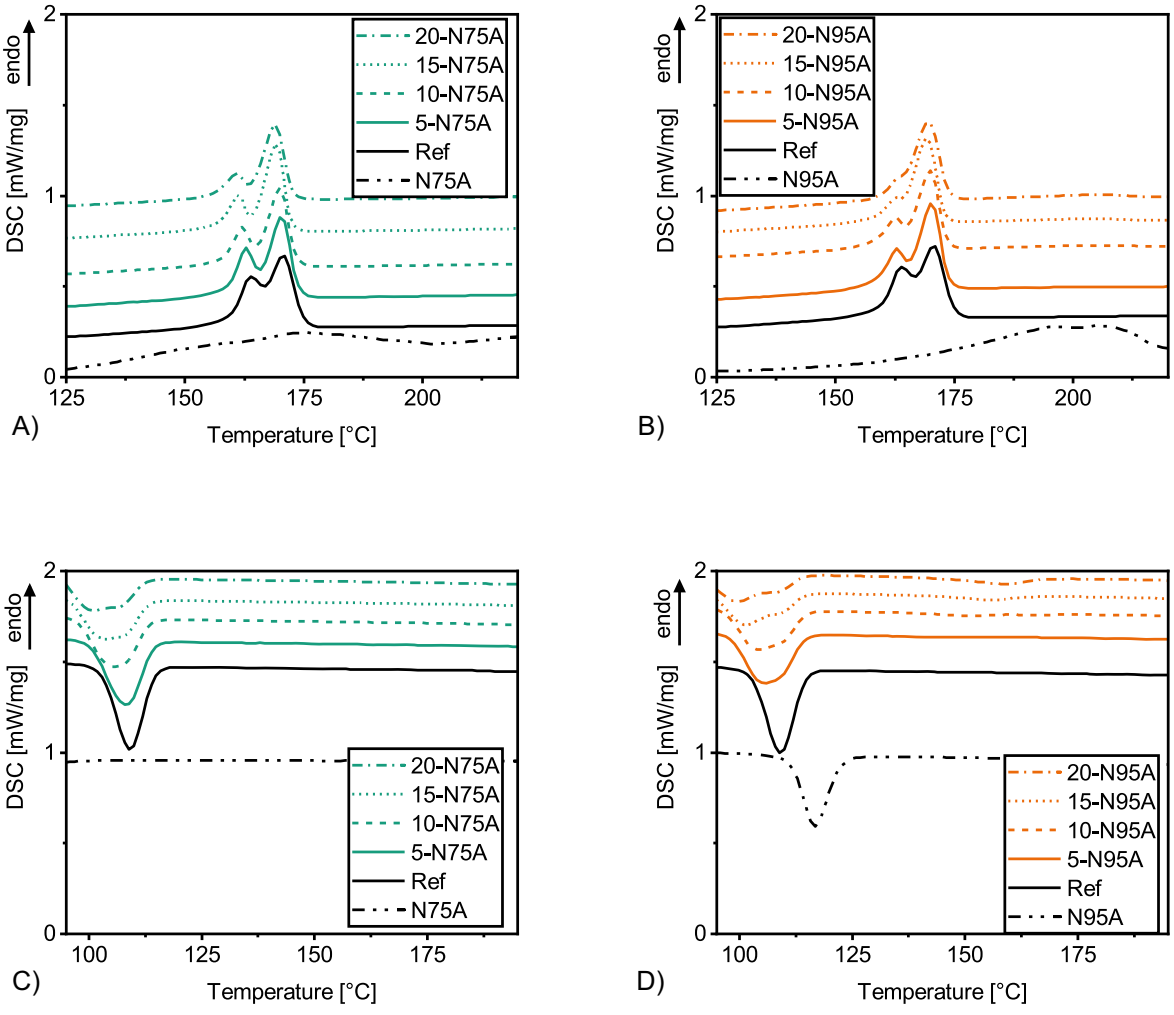

Figure 4: Close-ups of the DSC graphs of the produced compounds: Cooling (bottom) and second heating (top) curves of the samples containing N75A (A, C) and N95A (B, D).

content of the TPU. Thus, it can be concluded that the TPU partly inhibits the crystallization of the PLA phase. This leads to less, especially small, crystallites, which leads to the diminishing melting peak at around 163 °C. Another interesting detail is the fact that the TPU in the blend – in contrast to the pure TPU – neither crystallizes nor shows any melting behavior. This leads to the conclusion that the compatibility due to physical interactions between the PLA and the TPU seems to be quite good.

Table 6 shows the glass transition temperatures (T_g) of the compounds. It can be seen that the Tgs of the PLA are lower for the blends containing TPU compared to the pure reference material. This can also be explained by an interaction between PLA and the TPUs as observed from the findings of Bernardes et al. (Bernardes et al. 2020). Additionally, this is in accordance with the above mentioned results of the missing crystallization and melting peaks of TPU in the blends. For the blends containing N75A a steady decrease of T_g can be observed with increasing content of the TPU. This may be due to the fact that N75a contains a plasticizer which may also be miscible with PLA and thus leads to a decrease of its T_g. This behavior cannot be observed for the blends containing N95A, which also supports the plasticizer distribution hypothesis, because N95A does not contain any plasticizer.

It has to be noted that the second bio-based polymer, which is contained inside the PLA blend, also exhibits melting and crystallization phenomena. They do not change upon the addition of the TPUs and thus are not shown in detail.

Table 7 lists the MFIs of the produced compounds. It can be seen that the addition of the softer N75A does not show a significant impact on the MFI. As the results of the thermal properties revealed, the plasticizer of the N75A may also be miscible with PLA. This could lead to a lower viscosity of the matrix material, i.e. PLA, and thus a lower viscosity of the whole blend. At the same time, the higher viscosity of the TPU itself counteracts the influence of the plasticizer and thus no change in the viscosity of the blend can be observed. On the other side, the harder N95A significantly affects the viscosity and thus the MFI of the compounds. The MFI values steadily decrease with an increasing content of the N95A. When adding 20% of the N95A the value reaches a level of less than 1 g/10 min, which lies under a reasonable measurement limit. In total, the addition of the N95A leads to a significantly higher viscosity with increasing TPU content, while the addition of the softer N75A does not change the blend viscosity.

3.3 Surface and interfacial tension

The results of the DSA are shown in Table 8. While the contact angles of the almost nonpolar diiodomethane show stable values for every blend, the angles of the water change upon the addition of the TPU to the blend. With increasing amount of TPU, the contact angle decreases, which corresponds to an increasing wettability. This applies to both TPU materials. The calculated total SFE shows a steady increase with increasing amount of TPU in the blend. Although the dispersive component of the energy decreases, the total value of the SFE increases due to a higher gradient of the increase in the polar component. It is known that higher polar components of the SFE of a substrate material lead to higher bonding strengths (Mirabedini et al. 2004).

In Table 9 the calculated interfacial tensions between the corresponding material combinations are listed. From these results, the assumption can be made that N75A shows a higher adhesive bonding strength on the PLA reference material, than the N95A. The addition of TPU to the PLA blend enhances the adhesive surface properties of the created material by reducing the interfacial tension between the two components. For both TPU, the interfacial tension decreases with increasing soft component in the

Table 6: Glass transition temperatures of the compounded samples and the reference materials.

Sample	Ref	N75A	N95A	5-N75A	10-N75A	15-N75A	20-N75A	5-N95A	10-N95A	15-N95A	20-N95A
$T_{g,1}$ [°C]	–	−48.1	−26.2	−33.1	−31.8	−33.6	−33.9	−31.2	−30.4	−31.7	−30.9
$T_{g,2}$ [°C]	62.0	–	–	60.0	58.2	59.2	57.4	60.3	60.2	60.5	61.0

Table 7: Values of the measured melt flow indices (MFI).

Sample	Ref	5-N75A	10-N75A	15-N75A	20-N75A	5-N95A	10-N95A	15-N95A	20-N95A
MFI (210°C/2.16 kg) [g/10min]	28.7	30.0	29.7	27.3	26.5	19.7	8.2	3.7	<1

Table 8: Mean values and standard deviation of the measured contact angles and calculated surface free energy of the used materials.

	Contact angle		Surface free energy		
Sample	**Water [°]**	**Diiodomethane [°]**	**Polar [mN/m]**	**Dispersive [mN/m]**	**Total [mN/m]**
N75A	78.8 ± 3.2	55.6 ± 6.0	7.6	26.1	33.6
N95A	72.0 ± 4.0	52.6 ± 4.3	11.0	26.5	37.4
Ref	88.8 ± 1.6	51.8 ± 2.6	2.5	30.9	33.4
5-N75A	88.2 ± 2.2	51.1 ± 0.8	2.6	31.3	33.8
10-N75A	82.0 ± 1.6	51.0 ± 0.9	5.0	29.7	34.8
15-N75A	77.2 ± 2.4	51.1 ± 1.9	7.5	28.5	36.0
20-N75A	74.8 ± 3.1	51.7 ± 0.6	9.0	27.6	36.6
5-N95A	83.6 ± 1.6	51.5 ± 1.2	4.4	29.8	34.2
10-N95A	78.3 ± 2.8	51.7 ± 0.9	7.0	28.4	35.5
15-N95A	73.9 ± 3.1	51.6 ± 2.1	9.5	27.5	37.0
20-N95A	69.5 ± 2.1	51.7 ± 1.0	12.4	26.4	38.8

Table 9: Calculated interfacial tension and work of adhesion between the created blends (sample) and the two TPU (N75A and N95A).

	Interfacial tension [mN/m]	
Sample	**N75A**	**N95A**
Ref	1.59	3.19
5-N75A	1.56	–
10-N75A	0.38	–
15-N75A	0.05	–
20-N75A	0.08	–
5-N95A	–	1.57
10-N95A	–	0.47
15-N95A	–	0.06
20-N95A	–	0.05

hard component blend. In both cases the addition of 15 ma.% of the TPU to the PLA blend results in interfacial tensions close to zero, which in theory represents a high work of adhesion since the distance between the two components will be small enough for the bonding forces (e.g. van der Waals interactions) to act (Baldan 2012). Since other surface characteristics like the surface roughness of the substrate plate or the surface chemistry of the materials in contact can also affect the actual work of adhesion, the interfacial tension only provides basic information about the practical bonding strength of 2C material joints. Without further surface characterization, it only allows the comparison of different material combinations regarding their adhesive bonding abilities. Therefore, it is possible to analyze the impact of surface treatments or material modifications in comparison to the reference material.

3.4 Morphological properties

The blend morphology was investigated via SEM pictures of the cryo-fractured sample bars. Figure 5 depicts the corresponding surface of the blend containing 20% N75A. There are sheet shaped fillers inside the reference material that can be attributed to phyllosilicates. In addition to these fillers, small droplet-shaped inclusions can also be detected. Since the reference material itself is already a polymer blend of two bio-based polyesters, these inclusions cannot be entirely attributed to the TPU. Comparing the morphology of the different produced blends no change in shape or size of the inclusions can be observed. Furthermore, no correlation

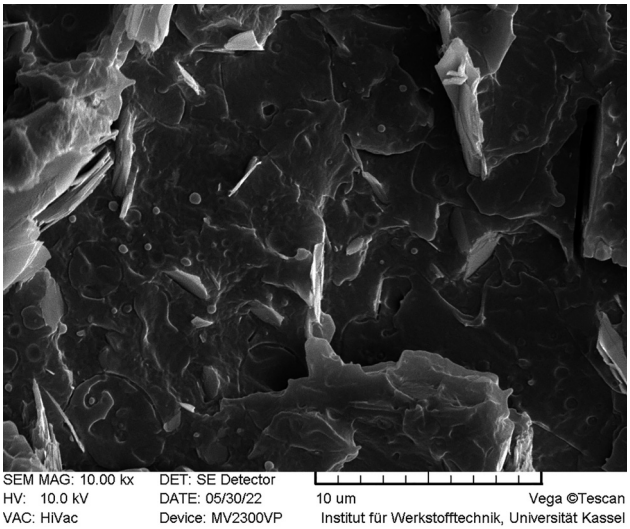

Figure 5: SEM picture of the cryo-fractured sample bar of 20-N75A.

between the amount of TPU in the blends and the number and distribution of inclusions can be established by the SEM images. Therefore, the other blend compositions are not shown here.

Bernardes et al. (Bernardes et al. 2020) found a clearly separated phase structure inside blends of PLA and TPU. Their blends contained visible TPU droplets in the size of around 4 µm for an uncompatibilized blend and of around 2 µm for a compatibilized blend using poly(ethylene-butyl acrylate-glycidyl methacrylate) as a compatibilizer. The droplets that are visible in Figure 5 are significantly smaller than the ones observed by Bernardes et al. This difference may be due to the fact that here injection molded test pieces were used and that a polyester-based TPU was used, which shows good compatibility with the polyesters inside the reference material. The small values of the calculated interfacial tensions between the two materials also support this assumption, indicating a good compatibility of the polymeric phases inside the blends.

3.5 Mechanical properties of the neat materials and the blends

Table 10 shows the mechanical properties of both TPUs. Compared to N95A, N75A only has about one third of the tensile strength but a much higher elongation at break. This difference affects the stress-strain behavior of the compounded blends. The blends containing N75A also show higher elongations at break with lower tensile strengths.

Compounding the reference material with the two types of TPU clearly affects the mechanical properties. Typically, blending of a soft and ductile elastomeric phase and a stiff and brittle thermoplastic polymer enhances the ductility of the latter (Zhao et al. 2020). This also applies for the blends compounded in this study. The values of the mechanical properties are listed in Table 11. Increasing the content of TPU inside the blends increases the elongation at break as well as the notched and unnotched impact strength.

On the other side, due to the TPU being a much softer polymer compared to PLA, the Young's Modulus as well as the tensile strength decrease accordingly, as depicted in Figure 6. It can be seen that for the blends containing the TPU with a higher shore-hardness, N95A, the Young's moduli as well as the tensile strengths are higher than those of the blends containing the softer TPU N75A.

The results of the mechanical properties are summarized graphically in Figure 7.

3.6 Peel test results

During peel tests, the measured force is plotted over the peel distance. For the N95A peel test specimens produced for this study, this plot shows a typical pattern, which can be seen in Figure 8 (right). Due to an unavoidable ridge on

Table 10: Mechanical properties of the two TPUs (mean values and standard deviation).

Sample	Tensile strength [MPa]	Elongation at break [%]	Stress at 100% elongation [MPa]	Stress at 300% elongation [MPa]	Hardness [Shore A]
N75A	10.8 ± 0.3	775.8 ± 43.9	4.1 ± 0.0	5.9 ± 0.0	75.8 ± 0.2
N95A	32.4 ± 2.0	423.1 ± 7.5	12.5 ± 0.1	16.1 ± 0.2	94.7 ± 0.2

Table 11: Mechanical properties of the compounded blends (mean values and standard deviation).

Sample	Young's modulus [MPa]	Tensile strength [MPa]	Elongation at break [%]	Charpy impact strength [kJ/m^2]	Charpy notched impact strength [kJ/m^2]
Ref	2762 ± 67	45.8 ± 0.5	4.6 ± 0.4	31 ± 2	2.3 ± 0.2
5-N75A	2386 ± 173	40.7 ± 0.9	6.6 ± 0.3	48 ± 8	3.0 ± 0.5
10-N75A	1971 ± 118	36.6 ± 0.6	11.4 ± 4.0	91 ± 13	4.3 ± 0.1
15-N75A	1687 ± 84	32.1 ± 0.6	20.6 ± 4.4	185 ± 36	5.6 ± 0.2
20-N75A	1520 ± 113	27.4 ± 0.5	39.5 ± 9.0	193 ± 4	7.3 ± 0.5
5-N95A	2524 ± 69	41.9 ± 0.7	6.3 ± 0.7	55 ± 9	2.8 ± 0.5
10-N95A	2136 ± 54	37.1 ± 0.3	8.1 ± 0.7	106 ± 10	4.2 ± 0.2
15-N95A	1900 ± 77	33.2 ± 0.4	10.4 ± 1.3	193 ± 38	4.9 ± 0.3
20-N95A	1645 ± 71	31.0 ± 0.4	15.5 ± 3.1	207 ± 41	6.0 ± 0.5

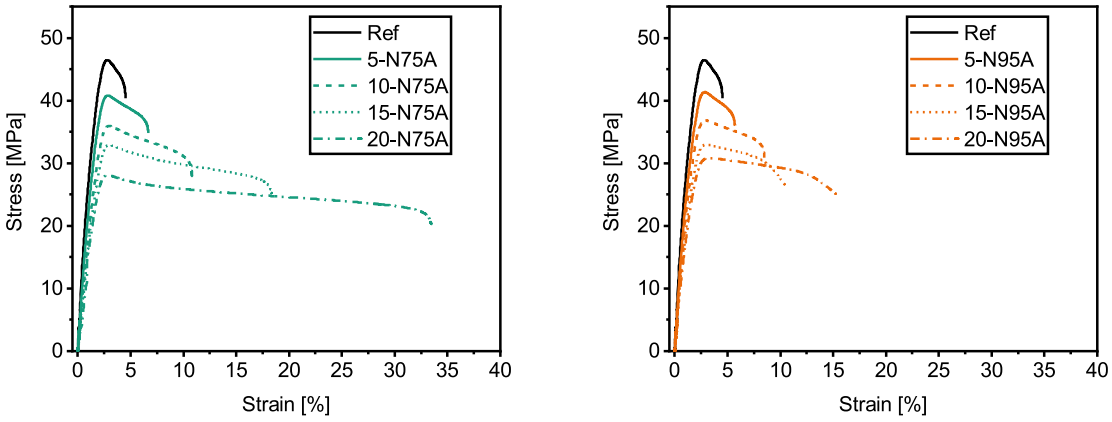

Figure 6: Stress-strain curves of the compounded blends N75A (left) and N95A (right).

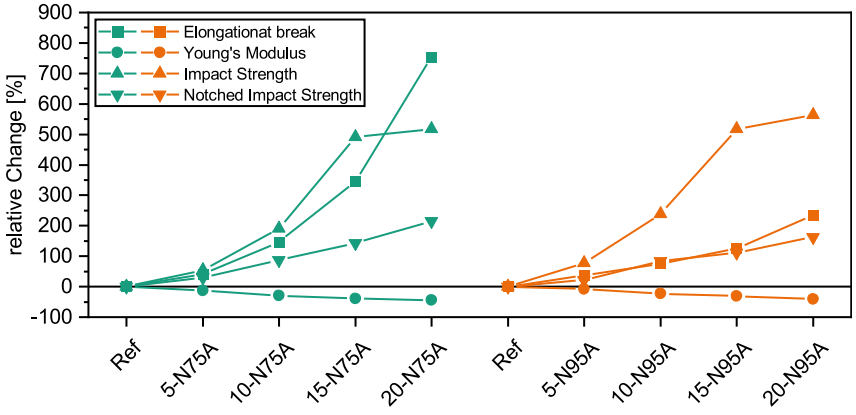

Figure 7: Relative change of the mechanical properties with regard to the formulation.

the specimen side where the TPU tab protrudes above the substrate plate, increased forces are required to begin the peeling. In the graph this effect is seen at a distance between 0 and 20 mm. A second peak occurs short before the end of the peel distance and is caused by an internal pressure sensor in the mold cavity. Therefore, the mean value of the peel force is calculated between a distance of 20 and 130 mm. The force-distance plots of the material combinations containing N75A (Figure 8, left) reveal a different pattern. Only the reference PLA blend shows an adhesive peeling, while for the others a cohesive failure of the soft component occurred. It means that the adhesive

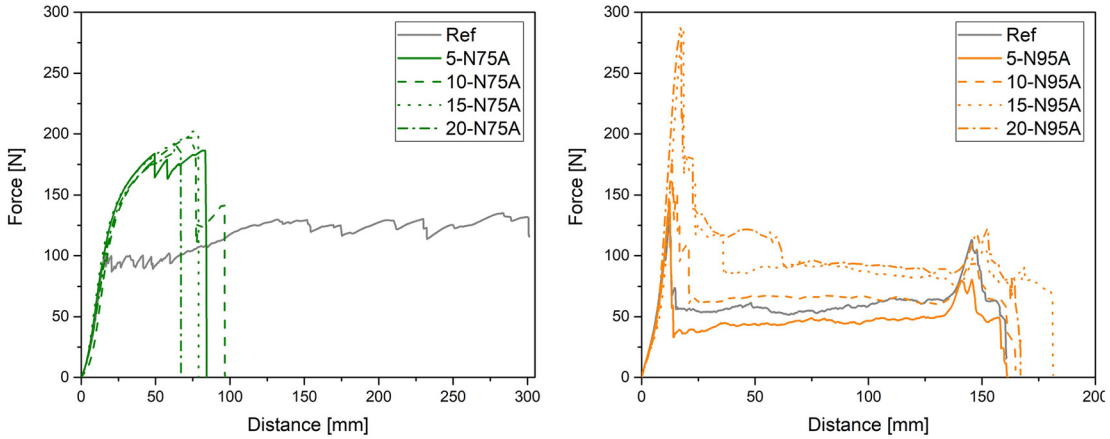

Figure 8: Force-distance curves of the compounded blends in combination with N75A (left) and N95A (right).

Table 12: Average peel forces and standard deviation of the compounded blends.

	Average peel force [N]	
Sample	**N75A**	**N95A**
Ref	118.4 ± 8.0	54.6 ± 3.1
5-N75A	177.9[a] ± 41.8	–
10-N75A	198.7[a] ± 3.6	–
15-N75A	199.1[a] ± 2.8	–
20-N75A	188.4[a] ± 3.8	–
5-N95A	–	47.3 ± 2.9
10-N95A	–	63.7 ± 6.0
15-N95A	–	93.3 ± 11.7
20-N95A	–	130.3 ± 76.1

[a]measured maximum force.

bonding strength of the material joints was higher than the tensile strength of the N75A. Since no statement about the actual bond strength can be made, only maximum measured forces are listed. The results of the peeling tests are given in Table 12.

While no conclusive statement on the effect of adding the soft component to enhance the adhesive bonding properties can be made for the compounded blends containing N75A, the blends containing N95A show a very clear positive effect. Although the addition of 5 wt% of N95A to the PLA reference material lowers the average peel force, this force increases significantly with higher amounts of the soft component in the blend. For the blends containing N75A, an addition of 5% soft component was enough to increase the adhesive bonding strength to the point where it was higher than the cohesive tensile strength of the TPU. The relative change of the polar part of the SFE, the IFT and the peel force are graphically summarized in Figure 9.

4 Conclusions

The results of the mechanical and morphological analysis reveal that the PLA reference material and the two used TPU types are compatible. The SEM images show small droplet-shaped inclusions but no large-scale phase separation and the Young's modulus and tensile strength of the blends follow a linear mixing rule with increasing TPU content. The DSC measurements reveal that the TPU phase inside the compounded blends does not show any crystallization and melting peaks but alleviates the crystallization of the PLA. This also indicates a good compatibility of the polymeric phases, due to the resulting interactions between them. By blending PLA with the different TPUs, the inherent brittleness of the PLA was reduced. Thus, a much more ductile hard component for the use in 2C injection molding was received. The elongation at break was around eight times that of the neat PLA blend and the notched impact strength was around three times higher as for the reference material. Furthermore, the compatibility of the materials also resulted in good processabilities. The processing parameters during the compounding and the injection molding did not have to be adjusted with increasing amount of TPU in the blends. Only the resulting mass temperature and the SMEC showed a slight increase for the blends containing the N95A, which can be traced back to a higher viscosity of the harder TPU.

The measured SFE of the compounded blends and the interfacial tension between them and the two TPU proof that an increasing amount of soft component in the blend enhances the wettability and adhesive properties of the substrate surfaces. The performed peel tests reveal that the improved surface properties result in higher bonding strengths, confirming the hypotheses shown in Figure 1.

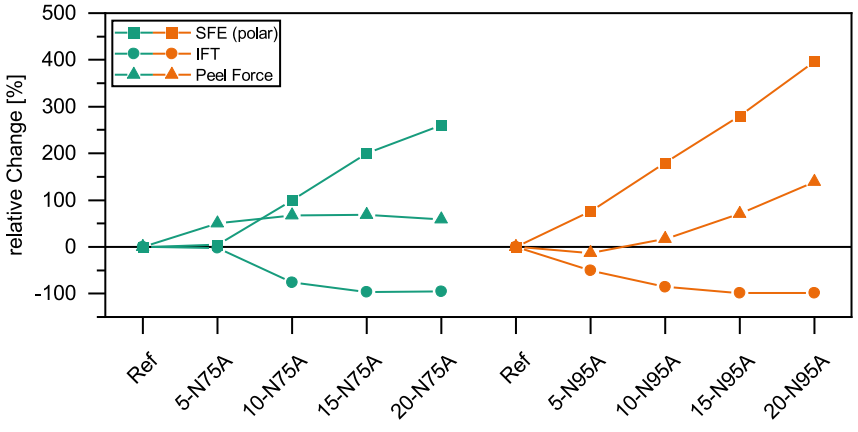

Figure 9: Relative change of the surface free energy (SFE), the interfacial tension (IFT) and the peel force with regard to the formulation.

While the bonding strength of the N95A combinations was increased by 140%, the adhesive bonds of the N75A combination were higher than the soft components' tensile strength, resulting in a cohesive failure.

Author contributions: All the authors have accepted responsibility for the entire content of this submitted manuscript and approved submission.

Research funding: This project was funded by the German Federal Ministry of Food and Agriculture (BMEL) within the "renewable resources" funding program from the Agency for Renewable Resources (FNR) (FKZ: 22000915, 22011816, 22011916).

Conflict of interest statement: The authors declare no conflict of interest.

References

Anakabe, J., Zaldua Huici, A.M., Eceiza, A., and Arbelaiz, A. (2015). Melt blending of polylactide and poly(methyl methacrylate): thermal and mechanical properties and phase morphology characterization. J. Appl. Polym. Sci. 132: 1–8, https://doi.org/10.1002/app.42677.

Baldan, A. (2012). Adhesion phenomena in bonded joints. Int. J. Adhes. Adhes. 38: 95–116, https://doi.org/10.1016/j.ijadhadh.2012.04.007.

Bernardes, G.P., Rosa Luiz, N., Santana, R.M.C., and Camargo Forte, M.M. (2020). Influence of the morphology and viscoelasticity on the thermomechanical properties of poly(lactic acid)/thermoplastic polyurethane blends compatibilized with ethylene-ester copolymer. J. Appl. Polym. Sci. 137: 48926, https://doi.org/10.1002/app.48926.

Cao, X., Dong, W., He, M., Zhang, J., Ren, F., and Li, Y. (2019). Effects of blending sequences and molecular structures of the compatibilizers on the morphology and properties of PLLA/ABS blends. RSC Adv. 9: 2189–2198, https://doi.org/10.1039/C8RA09193E.

Chen, D. and Zhen, W. (2021). Performance, interfacial compatibility testing and rheonaut technology analysis for simultaneous rheology and FTIR of poly(lactic acid)/modified saponite nanocomposites. Polym. Test. 100: 107232, https://doi.org/10.1016/j.polymertesting.2021.107232.

Di Bartolo, A., Infurna, G., and Dintcheva, N.T. (2021). A review of bioplastics and their adoption in the circular economy. Polymers 1–26, https://doi.org/10.3390/polym13081229.

European Bioplastics (2021). *Bioplastics market data*, Available at: https://www.european-bioplastics.org/market/ (Accessed 15 June 2021).

European Commission (2019). *The European green deal COM 640 final*, Available at: https://eur-lex.europa.eu/legal-content/EN/TXT/?uri=COM:2019:640:FIN (2019) (Accessed 15 June 2021).

Filho, W.L., Salvia, A.L., Bonoli, A., Saari, U.A., Voronova, V., Klõga, M., Kumbhar, S.S., Olszewski, K., de Quevedo, D.M., and Barbir, J. (2021). An assessment of attitudes towards plastics and bioplastics in Europe. Science of the total environment 755: 142732, https://doi.org/10.1016/j.scitotenv.2020.142732.

Fowkes, F.M. (1964). Attractive forces and interfaces. Ind. Eng. Chem. Res. 56: 40–52, https://doi.org/10.1021/ie50660a008.

Garlotta, D. (2001). A literature review of poly(lactic acid). J. Polym. Environ. 9: 63–84, https://doi.org/10.1023/A:1020200822435.

Gere, D. and Czigany, T. (2020). Future trends of plastic bottle recycling: compatibilization of PET and PLA. Polym. Test. 81: 106160, https://doi.org/10.1016/j.polymertesting.2019.106160.

Güzel, K., Klute, M., Kurgan, N., and Heim, H.-P. (2020). Influence of the degree of crystallinity and the surface free energy on the adhesion properties of different PLA/PBS blends in multicomponent injection molding. AIP Conference Proceedings 2205: 020019, https://doi.org/10.1063/1.5142934.

Hamad, K., Kaseem, M., Ayyoob, M., Joo, J., and Deri, F. (2018). Polylactic acid blends: the future of green, light and tough. Prog. Polym. Sci. 85: 83–127, https://doi.org/10.1016/j.progpolymsci.2018.07.001.

Institute for Bioplastics and Biocomposites (2020). Biopolymers, facts and statistics. IfBB – Institute for Bioplastics and Biocomposites, Hannover, https://www.ifbb-hannover.de/files/IfBB/downloads/faltblaetter_broschueren/f+s/Biopolymers-Facts-Statistics-2020.pdf.

Janczuk, B. and Bialopiotrowicz, T. (1989). Surface free-energy components of liquids and low energy solids and contact angles. J. Colloid Interface Sci. 127: 189–204.

Kaelble, D.H. (1970). Dispersion-polar surface tension properties of organic solids. J. Adhes. 2: 66–81, https://doi.org/10.1080/0021846708544582.

Kang, H., Lu, X., and Xu, Y. (2015). Properties of immiscible and ethylene-butyl acrylate-glycidyl methacrylate terpolymer compatibilized poly (lactic acid) and polypropylene blends. Polym. Test. 43: 173–181, https://doi.org/10.1016/j.polymertesting.2015.03.012.

Kloubek, J. (1992). Development of methods for surface free energy determination using contact angles of liquids and solids. Adv. Colloid Interface Sci. 38: 99–142, https://doi.org/10.1016/0001-8686(92)80044-x.

Klute, M., Feldmann, M., and Heim, H.-P. (2018). Bio-based alternatives for hard-soft connections. Kunstst. Int. 40: 44.

Mieth, F. and Tromm, M. (2016). Multicomponent technologies. In: *Specialized injection molding techniques*. Elsevier, pp. 1–51.

Mirabedini, S., Rahimi, H., Hamedifar, S., and Mohsen Mohseni, S. (2004). Microwave irradiation of polypropylene surface: a study on wettability and adhesion. Int. J. Adhes. 24: 163–170, https://doi.org/10.1016/j.ijadhadh.2003.09.004.

Nakajima, H., Dijkstra, P., and Loos, K. (2017). The recent developments in biobased polymers toward general and engineering applications: polymers that are upgraded from biodegradable polymers, analogous to petroleum-derived polymers, and newly developed. Polymers 9: 1–26, https://doi.org/10.3390/polym9100523.

Pilla, S. (2011). *Handbook of Bioplastics and Biocomposites engineering applications*. John Wiley & Sons, Hoboken, NJ, USA.

Piontek, A., Vernaez, O., and Kabasci, S. (2020). Compatibilization of poly(lactic acid) (PLA) and bio-based ethylene-propylene-diene-rubber (EPDM) via reactive extrusion with different coagents. Polymers 12: 1–21, https://doi.org/10.3390/polym12030605.

Przybysz-Romatowska, M., Haponiuk, J., and Formela, K. (2020). Poly(ε-Caprolactone)/Poly(Lactic acid) blends compatibilized by

peroxide initiators: comparison of two strategies. Polymers 12: 1–12, https://doi.org/10.3390/polym12010228.

Rasselet, D., Caro-Bretelle, A.-S., Taguet, A., and Lopez-Cuesta, J.-M. (2019). Reactive compatibilization of PLA/PA11 blends and their application in additive manufacturing. Mater 12: 1–18, https://doi.org/10.3390/ma12030485.

Rauwendaal, C. (2014). *Polymer extrusion*, 5th ed. München: Hanser.

Rüppel, A. (2021). *Untersuchung von Flüssigsilikonkautschuk-Polypropylen-Verbunden - Einflüsse der Lagerung und des Verarbeitungsprozesses auf die Haftungseigenschaften*, Dissertation, Universität Kassel, Kassel, Germany.

Rüppel, A., Giesen, R.-U., and Heim, H.-P. (2017). The adhesion of LSR thermoplastic composites after storage tests. SPE ANTEC® 138: 142.

Schlitt, C.U., Hartung, M., Rüppel, A., Giesen, R.-U., and Heim, H.-P. (2019). UV pre-treatment for polycarbonate for bonding LSR in a multi-component injection molding process. Int. Polym. Proc. 34: 30–36, https://doi.org/10.3139/217.3509.

Spierling, S., Knüpffer, E., Behnsen, H., Mudersbach, M., Krieg, H., Springer, S., Albrecht, S., Herrmann, C., and Endres, H.-J. (2018). Bio-based plastics - a review of environmental, social and economic impact assessments. J. Clean. Prod. 185: 476–491, https://doi.org/10.1016/j.jclepro.2018.03.014.

Su, S., Kopitzky, R., Tolga, S., and Kabasci, S. (2019). Polylactide (PLA) and its blends with poly(butylene succinate) (PBS): a brief review. Polymers 11: 1–21, https://doi.org/10.3390/polym11071193.

United Nations (2015). *Transforming our world: the 2030 Agenda for sustainable development*, Available at: https://sdgs.un.org/2030agenda (Accessed 15 June 2021).

Wang, R., Zhang, J., Kang, H., and Zhang, L. (2016a). Design, preparation and properties of bio-based elastomer composites aiming at engineering applications. Compos. Sci. Technol. 133: 136–156, https://doi.org/10.1016/j.compscitech.2016.07.019.

Wang, S., Pang, S., Pan, L., Xu, N., and Li, T. (2016b). Isothermal cold crystallization, heat resistance, and tensile performance of polylactide/thermoplastic polyester elastomer (PLA/TPEE) blends: effects of annealing and reactive compatibilizer. Polymers 8: 1–16, https://doi.org/10.3390/polym8120417.

Yokohara, T. and Yamaguchi, M. (2008). Structure and properties for biomass-based polyester blends of PLA and PBS. Eur. Polym. J. 44: 677–685, https://doi.org/10.1016/j.eurpolymj.2008.01.008.

Zhao, X., Hu, H., Wang, X., Yu, X., Zhou, W., and Peng, S. (2020). Super tough poly(lactic acid) blends: a comprehensive review. RSC Adv. 10: 13316–13368, https://doi.org/10.1039/D0RA01801E.